Ceramics International 49 (2023) 1–40

CERAMICS INTERNATIONAL

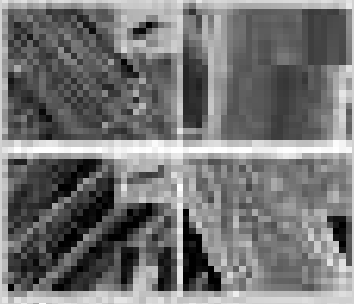

Submit Your Paper

Supports Open Access (https://www.elsevier.com/journals/ceramics-international/0272-8842/open-access-options)

View Articles (https://www.sciencedirect.com/science/journal/02728842)

Guide for Authors

Abstracting/ Indexing (http://www.elsevier.com/journals/ceramics-international/0272-8842/abstracting-indexing)

Track Your Paper

Order Journal (https://www.elsevier.com/journals/institutional/ceramics-international/0272-8842)

Journal Metrics

› CiteScore: **6.1**

Impact Factor: **3.830**

5-Year Impact Factor: **3.513**

Source Normalized Impact per Paper (SNIP): **1.310**

SCImago Journal Rank (SJR): **0.891**

› View More on Journal Insights

Your Research Data

› Share your research data (https://www.elsevier.com/authors/author-resources/research-data)

Related Links

› Author Stats

› Researcher Academy

› Author Resources (https://www.elsevier.com/authors/author-resources)

› Try out personalized alert features

Ceramics International - Editorial Board

General Editor

P. Vincenzini

World Academy of Ceramics, National Research Council, Faenza, Italy

Editors-in-Chief

R.K. Bordia

Clemson University, Clemson, South Carolina, United States

Z.Y. Fu

Ministry of Education of the Peoples Republic of China Changjiang Scholar Program, Wuhan, China

T. Ohji

National Institute of Advanced Industrial Science and Technology Advanced Manufacturing Research Institute, Tsukuba, Japan

V.C. Pandolfelli (https://www.journals.elsevier.com:443/ceramics-international/editorial-board/vc-pandolfelli)
Federal University of Sao Carlos Department of Materials Engineering, SAO CARLOS, Brazil

R. Riedel

Technical University of Darmstadt Department of Materials and Earth Sciences, Darmstadt, Germany

Associate Editor

Z.J. Yu

Xiamen University, Xiamen, China

Editorial Board

National Institute for Materials Science, 305-0044, Tsukuba-Shi, Japan

Z.J. Shen
Stockholm University Department of Materials and Environmental Chemistry, S-106 91, Stockholm, Sweden

W. Sigmund
University of Florida Department of Materials Science and Engineering, 225 Rhines Hall, P.O. Box 116400, Gainesville, Florida, 32611-6400, United States

M. Singh
NASA John H Glenn Research Center, MS 106-5 Ceramic Branch, Cleveland, Ohio, OH 44135-3191, United States

G. Srinivasan
Oakland University, Rochester, Michigan, 48309-4401, United States

D. Suvorov
Jozef Stefan Institute, 1000, Ljubljana, Slovenia

T. Troczynski
The University of British Columbia, Vancouver, V6T 1Z4, British Columbia, Canada

W.H. Tuan
National Taiwan University Department of Materials and Science Engineering, No. 1, Sec. 4, Roosevelt Road, 10617, Taipei, Taiwan

A. Vinu
Newcastle University, NE1 7RU, Newcastle, United Kingdom

M. Wang
Tongji University College of Design and Innovation, Shanghai, China

S. Yin
Tohoku University, 2-1-1 Katahira, Aoba-ku, 980-8577, Sendai, Japan

N. Zhou
Henan University of Technology, Luoyang, China

Y. Zhou
Chinese Academy of Sciences, China

Y. Zhou
Harbin Institute of Technology Institute of Advanced Ceramics, 92 West Dazhi Street, Nan'gang District, 150001, Harbin, China

Ceramics International

Readers
View Articles

Ceramics International

Volume 46, Issue 5

Pages 5507-7000 (1 April 2020)

Previous vol/issue
Next vol/issue

Actions for 100 selected articles

Contents

Set up journal alerts

1. Reviews

1. ☑ select article Doped ZnO nanostructures with selected elements - Structural, morphology and optical properties: A review

   Review articleAbstract only

   Doped ZnO nanostructures with selected elements - Structural, morphology and optical properties: A review

   Boshra Ghanbari Shohany, Ali Khorsand Zak
   Pages 5507-5520
   View PDF
   Article preview

2. ☑ select article Review of perovskite-structure related cathode materials for solid oxide fuel cells

   Review articleAbstract only

   Review of perovskite-structure related cathode materials for solid oxide fuel cells

   Paramvir Kaur, K. Singh
   Pages 5521-5535
   View PDF
   Article preview

3. ☑ select article Wood-derived ultra-high temperature carbides and their composites: A review

   Review articleAbstract only

   Wood-derived ultra-high temperature carbides and their composites: A review

   Min Yu, Guo-jun Zhang, Theo Saunders
   Pages 5536-5547
   View PDF
   Article preview

2. Original Articles

1. ☑ select article Qualitative description on channel cracking in ceramic type coatings due to substrate tension using 3D discrete element method

   Research articleAbstract only

   Qualitative description on channel cracking in ceramic type coatings due to substrate tension using 3D discrete element method

   M.A. Ghasemi, S.R. Falahatgar
   Pages 5548-5565
   View PDF
   Article preview

2. ☑ select article Ternary ZnO/ZnAl₂O₄/ Al₂O₃ composite nanofiber as photocatalyst for conversion of CO₂ and CH₄

   Research articleAbstract only

   Ternary ZnO/$ZnAl_2O_4$/ Al_2O_3 composite nanofiber as photocatalyst for conversion of CO_2 and CH_4

   Pouran Moradipour, Farzad Dabirian, Mahsa Moradipour
   Pages 5566-5574
   View PDF
   Article preview

3. ☑ select article The formation mechanism of pores and unbonding in the Al₂O₃/Al₂O₃ joints brazed by 50Bi₂O₃–35B₂O₃–15ZnO glass

   Research articleAbstract only

   The formation mechanism of pores and unbonding in the Al_2O_3/Al_2O_3 joints brazed by $50Bi_2O_3$–$35B_2O_3$–15ZnO glass

   Wenhang Niu, Qianqian Chen, Panpan Lin, Jingyi Cui, ... Xiaoming Duan
   Pages 5575-5585
   View PDF
   Article preview

4. ☑ select article Preparation and formation mechanism of C/C–SiC composites using polymer-Si slurry reactive melt infiltration

Research articleAbstract only

Preparation and formation mechanism of C/C–SiC composites using polymer-Si slurry reactive melt infiltration

Wenjian Guo, Yicong Ye, Shuxin Bai, Li'an Zhu, Shun Li
Pages 5586-5593
View PDF
Article preview

5. ☑ select article Processing and thermal characterization of polymer derived SiCN(O) and SiOC reticulated foams

Research articleAbstract only

Processing and thermal characterization of polymer derived SiCN(O) and SiOC reticulated foams

Balanand Santhosh, Cekdar Vakifahmetoglu, Emanuel Ionescu, Andreas Reitz, ... Gian Domenico Sorarù
Pages 5594-5601
View PDF
Article preview

6. ☑ select article Characteristics of polycarbosilanes produced under different synthetic conditions and their influence on SiC fibers: Part I

Research articleAbstract only

Characteristics of polycarbosilanes produced under different synthetic conditions and their influence on SiC fibers: Part I

Seokhun Jang, Seong Gun Bae, Dong-Geun Shin, Kwangyoun Cho, ... Yoonjoo Lee
Pages 5602-5609
View PDF
Article preview

7. ☑ select article Low-temperature exfoliated graphene oxide incorporated with different types of natural rubber latex: Electrical and morphological properties and its capacitance performance

Research articleAbstract only

Low-temperature exfoliated graphene oxide incorporated with different types of natural rubber latex: Electrical and morphological properties and its capacitance performance

M.D. Nurhafizah, A.A. Aziz, A.B. Suriani, A. Mohamed, T. Soga
Pages 5610-5622
View PDF
Article preview

8. ☑ select article Material removal and interactions between an abrasive and a SiC substrate: A molecular dynamics simulation study

Research articleAbstract only

Material removal and interactions between an abrasive and a SiC substrate: A molecular dynamics simulation study

Van-Thuc Nguyen, Te-Hua Fang
Pages 5623-5633
View PDF
Article preview

9. ☑ select article Silver diffusion and mechanism of CaO-MgO-SiO₂ glass ceramics in millimeter-wave properties

Research articleAbstract only

Silver diffusion and mechanism of CaO-MgO-SiO_2 glass ceramics in millimeter-wave properties

Kuei-Chih Feng, Ming-Wei Chu, Chun-An Lu, Yoshiyuki Iizuka, ... Chung-Ya Tsao
Pages 5634-5640
View PDF
Article preview

10. ☑ select article Full characterization for material constants of a promising KNN-based lead-free piezoelectric ceramic

Research articleAbstract only

Full characterization for material constants of a promising KNN-based lead-free piezoelectric ceramic

Liao Qiao, Guo Li, Hong Tao, Jiagang Wu, ... Fei Li
Pages 5641-5644
View PDF

Article preview

11. ☑ select article Thermal stability and heat flux investigation of neutron-irradiated nanocrystalline silicon carbide (3C–SiC) using DSC spectroscopy

Research articleAbstract only

Thermal stability and heat flux investigation of neutron-irradiated nanocrystalline silicon carbide (3C–SiC) using DSC spectroscopy

Elchin M. Huseynov
Pages 5645-5648
View PDF
Article preview

12. ☑ select article Experimental investigation on high temperature wettability and structural behaviour of SAW fluxes using MgO–TiO₂ –SiO₂ and Al₂O₃–MgO–SiO₂ flux system

Research articleAbstract only

Experimental investigation on high temperature wettability and structural behaviour of SAW fluxes using $MgO–TiO_2–SiO_2$ and $Al_2O_3–MgO–SiO_2$ flux system

Lochan Sharma, Jagdish Kumar, Rahul Chhibber
Pages 5649-5657
View PDF
Article preview

13. ☑ select article Modulations in relaxor nature due to Sr²⁺ doping in 0.68PMN-0.32PT ceramic

Research articleOpen access

Modulations in relaxor nature due to Sr^{2+} doping in 0.68PMN-0.32PT ceramic

Pius Augustine, Muralidhar Miryala, Shibnath Samanta, S. Pavan Kumar Naik, ... M.S. Ramachandra Rao
Pages 5658-5664
Download PDF
Article preview

14. ☑ select article Local structure and evolution of phase transformation in Bi_{0.4871}Na_{0.4871}La_{0.0172}TiO₃–BaTiO₃ materials

Research articleAbstract only

Local structure and evolution of phase transformation in $Bi_{0.4871}Na_{0.4871}La_{0.0172}TiO_3–BaTiO_3$ materials

Atipong Bootchanont, Thanachai Boonchuduang, Atchara Khamkongkaeo, Thanit Saisopa, ... Rattikorn Yimnirun
Pages 5665-5670
View PDF
Article preview

15. ☑ select article Effect of defect states in the optical and magnetic properties of nanocrystalline NiO synthesised in a single step by an aerosol process

Research articleAbstract only

Effect of defect states in the optical and magnetic properties of nanocrystalline NiO synthesised in a single step by an aerosol process

Nandhini J. Usharani, S.S. Bhattacharya
Pages 5671-5680
View PDF
Article preview

16. ☑ select article High energy storage density and stable fatigue resistance of Na_{0.46}Bi_{0.46}Ba_{0.05}La_{0.02}Zr_{0.03}Ti_{0.97-x}Sn<sub>x</s ceramics

Research articleAbstract only

High energy storage density and stable fatigue resistance of $Na_{0.46}Bi_{0.46}Ba_{0.05}La_{0.02}Zr_{0.03}Ti_{0.97-x}Sn_xO_3$ ceramics

Arun Kumar Yadav, Huiqing Fan, Benben Yan, Chao Wang, ... Shuren Wang
Pages 5681-5688
View PDF
Article preview

17. ☑ select article Preparation, microstructure and electrical property of GdSmZr₂O₇-(Li₀_.₅₂Na_{0.48})₂CO₃ composite electrolyte via carbonate infiltration

Research articleAbstract only

Preparation, microstructure and electrical property of $GdSmZr_2O_7$-$(Li_{0.52}Na_{0.48})_2CO_3$ composite electrolyte via carbonate infiltration

Yu-Jun Jin, Zhan-Guo Liu, Zhao-Ying Ding, Gui Cao, Jia-Hu Ouyang
Pages 5689-5694
View PDF
Article preview

18. ☑ select article Study on the three-dimensional topography of the machined surface in laser-assisted machining of Si₃N₄ ceramics under different material removal modes

Research articleAbstract only

Study on the three-dimensional topography of the machined surface in laser-assisted machining of Si_3N_4 ceramics under different material removal modes

Yezhuang Pu, Yugang Zhao, Haiyun Zhang, Guoyong Zhao, ... Panpan Song
Pages 5695-5705
View PDF
Article preview

19. ☑ select article Flower-shaped ZnO nanomaterials for low-temperature operations in NO_X gas sensors

Research articleAbstract only

Flower-shaped ZnO nanomaterials for low-temperature operations in NO_X gas sensors

Srijita Nundy, Tae-yil Eom, Jun-gu Kang, Jaehyun Suh, ... Hoo-Jeong Lee
Pages 5706-5714
View PDF
Article preview

20. ☑ select article On the electric conduction of ZrO₂ in the steady stage of flash sintering

Research articleAbstract only

On the electric conduction of ZrO_2 in the steady stage of flash sintering

Shichen Lu, Jinling Liu, Gang Shao, Wen Liu, ... Linan An
Pages 5715-5718
View PDF
Article preview

21. ☑ select article Effects of B₂O₃–Li₂CO₃–SiO₂–ZnO glass on properties of Li_{0.43}Zn_{0.27}Ti_{0.13}Fe_{2.17}O₄ ferrites sintered at low temperatures

Research articleAbstract only

Effects of B_2O_3–Li_2CO_3–SiO_2–ZnO glass on properties of $Li_{0.43}Zn_{0.27}Ti_{0.13}Fe_{2.17}O_4$ ferrites sintered at low temperatures

Xiaoyi Wang, Zhiyong Zhong, Zhenwei Chen, Huaiwu Zhang, ... Yulong Liao
Pages 5719-5724
View PDF
Article preview

22. ☑ select article Enhanced photocatalytic hydrogen evolution over TiO₂/g-C₃N₄ 2D heterojunction coupled with plasmon Ag nanoparticles

Research articleAbstract only

Enhanced photocatalytic hydrogen evolution over TiO_2/g-C_3N_4 2D heterojunction coupled with plasmon Ag nanoparticles

Yuhao Yang, Chan Lu, Juan Ren, Xiaolong Li, ... Xia Zhao
Pages 5725-5732
View PDF
Article preview

23. ☑ select article The superlattice structure and self-adaptive performance of C–Ti/MoS₂ composite coatings

Research articleAbstract only

The superlattice structure and self-adaptive performance of C–Ti/MoS_2 composite coatings

Li Li, Zhaoxia Lu, Jibin Pu, Haixin Wang, ... Liping Wang
Pages 5733-5744
View PDF
Article preview

24. ☑ select article Effect of Mo addition mode on the microstructure and mechanical properties of TiC–high Mn steel cermets

Research articleAbstract only

Effect of Mo addition mode on the microstructure and mechanical properties of TiC–high Mn steel cermets

Guoping Li, Jixiang Jia, Yinghai Lyu, Jiazheng Zhao, ... Fenghua Luo
Pages 5745-5752
View PDF
Article preview

25. ☑ select article Effects of TiO₂ additive on ultra-low-loss MgO–LiF microwave dielectric ceramics

Research articleAbstract only

Effects of TiO_2 additive on ultra-low-loss MgO–LiF microwave dielectric ceramics

Zhenyu Tan, Huixing Lin, Kaixin Song, Mingzhao Dang, ... Haiyi Peng
Pages 5753-5756
View PDF
Article preview

26. ☑ select article Synthesis of red mud derived M-type barium hexaferrites with tuneable coercivity

Research articleAbstract only

Synthesis of red mud derived M-type barium hexaferrites with tuneable coercivity

João Carvalheiras, Rui M. Novais, Farzin Mohseni, João S. Amaral, ... Robert C. Pullar
Pages 5757-5764
View PDF
Article preview

27. ☑ select article Plasma-enhanced atomic layer deposition of gallium nitride thin films on fluorine-doped tin oxide glass substrate for future photovoltaic application

Research articleAbstract only

Plasma-enhanced atomic layer deposition of gallium nitride thin films on fluorine-doped tin oxide glass substrate for future photovoltaic application

Peng Qiu, Huiyun Wei, Yunlai An, Qixin Wu, ... Xinhe Zheng
Pages 5765-5772
View PDF
Article preview

28. ☑ select article Combined role of SiC particles and SiC whiskers on the characteristics of spark plasma sintered ZrB₂ ceramics

Research articleAbstract only

Combined role of SiC particles and SiC whiskers on the characteristics of spark plasma sintered ZrB_2 ceramics

Yaghoub Pazhouhanfar, Abbas Sabahi Namini, Shahrzad Shaddel, Zohre Ahmadi, Mehdi Shahedi Asl
Pages 5773-5778
View PDF
Article preview

29. ☑ select article Effect of Al₂O₃ particles on mechanical and tribological properties of Al–Mg dual-matrix nanocomposites

Research articleAbstract only

Effect of Al_2O_3 particles on mechanical and tribological properties of Al–Mg dual-matrix nanocomposites

M.A. Eltaher, A.Wagih, A. Melaibari, A. Fathy, G. Lubineau
Pages 5779-5787
View PDF
Article preview

30. ☑ select article The effect of Ag nanoparticles content on dielectric and microwave absorption properties of β-SiC

Research articleAbstract only

The effect of Ag nanoparticles content on dielectric and microwave absorption properties of β-SiC

Bo Wei, Jintang Zhou, Zhengjun Yao, Azhar Ali Haidry, ... Wenjing Chen
Pages 5788-5798
View PDF
Article preview

31. ☑ select article Influence of carbonation on the low-temperature consolidation by Spark Plasma Sintering of carbonated calcium phosphate bioceramics

Research articleAbstract only

Influence of carbonation on the low-temperature consolidation by Spark Plasma Sintering of carbonated calcium phosphate bioceramics

C. Ortali, I. Julien, C. Drouet, E. Champion
Pages 5799-5810
View PDF
Article preview

32. ☑ select article Nano-porous carbon materials derived from different biomasses for high performance supercapacitors

Research articleAbstract only

Nano-porous carbon materials derived from different biomasses for high performance supercapacitors

Huafang Yang, Xiaoyan Sun, Han Zhu, Yimin Yu, ... Qitu Zhang
Pages 5811-5820
View PDF
Article preview

33. ☑ select article Mn_xCo_{3-x}O₄ spinel coatings: Controlled synthesis and high temperature oxidation resistance behavior

Research articleAbstract only

$Mn_xCo_{3-x}O_4$ spinel coatings: Controlled synthesis and high temperature oxidation resistance behavior

Zhengjun Shen, Ju Rong, Xiaohua Yu
Pages 5821-5827
View PDF
Article preview

34. ☑ select article Dielectric, thermal and mechanical properties of hybrid PMMA/RGO/Fe₂O₃ nanocomposites fabricated by in-situ polymerization

Research articleAbstract only

Dielectric, thermal and mechanical properties of hybrid PMMA/RGO/Fe_2O_3 nanocomposites fabricated by in-situ polymerization

Yasir Ul-Haq, Imran Murtaza, Sadaf Mazhar, Rizwan Ullah, ... Shahid Amin
Pages 5828-5840
View PDF
Article preview

35. ☑ select article Study of (La,Sr)(Ti,Ni)O_{3-δ} materials for symmetrical Solid Oxide Cell electrode - Part B: Conditions of Ni exsolution

Research articleAbstract only

Study of $(La,Sr)(Ti,Ni)O_{3-\delta}$ materials for symmetrical Solid Oxide Cell electrode - Part B: Conditions of Ni exsolution

Charline Arrivé, Thibaud Delahaye, Olivier Joubert, Gilles H. Gauthier
Pages 5841-5849
View PDF
Article preview

36. ☑ select article Size controlled synthesis of well-distributed nano-silver on hydroxyapatite using alkanolamine compounds

Research articleAbstract only

Size controlled synthesis of well-distributed nano-silver on hydroxyapatite using alkanolamine compounds

Arniati Labanni, Zulhadjri, Dian Handayani, Yutaka Ohya, Syukri Arief
Pages 5850-5855
View PDF
Article preview

37. ☑ select article AlB₁₂-AlB₁₂C₂-TiB₂ hard and tough composites synthesized by reactive plasma activated sintering

Research articleAbstract only

AlB_{12}-$AlB_{12}C_2$-TiB_2 hard and tough composites synthesized by reactive plasma activated sintering

Guoqiang Luo, Peng Fan, Kejia Kang, Rong Tu, ... Lianmeng Zhang
Pages 5856-5862
View PDF
Article preview

38. ☑ select article Green emitting Ba_{1.5}Lu_{1.5}Al_{3.5}Si_{1.5}O₁₂: Ce³⁺ phosphor with high thermal emission stability for warm WLEDs and FEDs

Research articleAbstract only

Green emitting $Ba_{1.5}Lu_{1.5}Al_{3.5}Si_{1.5}O_{12}$: Ce^{3+} phosphor with high thermal emission stability for warm WLEDs and FEDs

Xiaoshuang Li, Chengjue Guo, Hongwei Wang, Yeqing Chen, ... Qingguang Zeng
Pages 5863-5870
View PDF
Article preview

39. ☑ select article Local atomic disorder and temperature dependence of saturation magnetization in yttrium iron garnet

Research articleAbstract only

Local atomic disorder and temperature dependence of saturation magnetization in yttrium iron garnet

R. Peña-Garcia, Y. Guerra, D.M. Oliveira, A. Franco, E. Padrón-Hernández
Pages 5871-5875
View PDF
Article preview

40. ☑ select article New observations on wear characteristics of solid Al₂O₃/Si₃N₄ ceramic tool in high speed milling of additive manufactured Ti6Al4V

Research articleAbstract only

New observations on wear characteristics of solid Al_2O_3/Si_3N_4 ceramic tool in high speed milling of additive manufactured Ti6Al4V

Jiaqiang Dang, Heng Zhang, Weiwei Ming, Qinglong An, Ming Chen
Pages 5876-5886
View PDF
Article preview

41. ☑ select article Optimizing graphene-TiO₂ interface properties via Fermi level modulation for photocatalytic degradation of volatile organic compounds

Research articleAbstract only

Optimizing graphene-TiO_2 interface properties via Fermi level modulation for photocatalytic degradation of volatile organic compounds

Zhen Zhou, Junxian Gao, Guangsheng Zhang, Yuming Dong, ... Jinze Lyu
Pages 5887-5893
View PDF
Article preview

42. ☑ select article Electrical and impedance spectroscopy properties of hydrothermally synthesized Ba_{0.2}Sr_{0.8-y}La_yFe₁₂O₁₉ (y = 0.2–0.8) nanorods

Research articleAbstract only

Electrical and impedance spectroscopy properties of hydrothermally synthesized $Ba_{0.2}Sr_{0.8-y}La_yFe_{12}O_{19}$ (y = 0.2–0.8) nanorods

N. Raghuram, T. Subba Rao, K. Chandra Babu Naidu
Pages 5894-5906
View PDF

Article preview

43. ☑ select article Incompatible magnetic and dielectric properties of BiCu_{3-x}Mn_xTi_{4-y}M_yO₁₂ (x = 0 & 0.5; y = 1 & 1.5 and M = Fe & Mn)

Research articleAbstract only

Incompatible magnetic and dielectric properties of $BiCu_{3-x}Mn_xTi_{4-y}M_yO_{12}$ (x = 0 & 0.5; y = 1 & 1.5 and M = Fe & Mn)

Ariful Haque, Ashish Shukla, Uma Dutta, Debamalya Ghosh, ... Md Motin Seikh
Pages 5907-5912
View PDF
Article preview

44. ☑ select article Synthesis and characterization of GaNb₁₁O₂₉@C for high-performance lithium-ion battery

Research articleAbstract only

Synthesis and characterization of $GaNb_{11}O_{29}$@C for high-performance lithium-ion battery

Zhen Wang, Runtian Zheng, Yuhang Li, Haoxiang Yu, ... Jie Shu
Pages 5913-5919
View PDF
Article preview

45. ☑ select article Structural, dielectric and magnetic properties of (ZnFe₂O₄/Polystyrene) nanocomposites synthesized by micro-emuslion technique

Research articleAbstract only

Structural, dielectric and magnetic properties of ($ZnFe_2O_4$/Polystyrene) nanocomposites synthesized by micro-emuslion technique

Qaiser Abbas, G. Murtaza, Nawaz Muhammad, Mohsin Ishfaq, ... Muhammad Zahir Iqbal
Pages 5920-5928
View PDF
Article preview

46. ☑ select article Al₂O₃–CaO macroporous ceramics containing hydrocalumite-like phases

Research articleAbstract only

Al_2O_3–CaO macroporous ceramics containing hydrocalumite-like phases

O.H. Borges, T. Santos, V.R. Salvini, V.C. Pandolfelli
Pages 5929-5936
View PDF
Article preview

47. ☑ select article Microstructure and mechanical property of SiC whisker coating modified C/C composite/Ti₂AlNb alloy dissimilar joints prepared by transient liquid phase diffusion bonding

Research articleAbstract only

Microstructure and mechanical property of SiC whisker coating modified C/C composite/Ti_2AlNb alloy dissimilar joints prepared by transient liquid phase diffusion bonding

Wang Jie, Feng Yang, Zhang Fuqi, Xiong Qinglian, ... Xiong Qinghai
Pages 5937-5945
View PDF
Article preview

48. ☑ select article Microstructure and interface-adhesion of thermally sprayed continuous gradient elastic modulus FeCrAl-ceramic coatings

Research articleAbstract only

Microstructure and interface-adhesion of thermally sprayed continuous gradient elastic modulus FeCrAl-ceramic coatings

Qiaolei Li, Chunming Deng, Lu Li, Jianguo Lü, ... Jiansheng Lu
Pages 5946-5959
View PDF
Article preview

49. ☑ select article Lychee-like ZnO/ZnFe₂O₄ core-shell hollow microsphere for improving acetone gas sensing performance

Research articleAbstract only

Lychee-like ZnO/$ZnFe_2O_4$ core-shell hollow microsphere for improving acetone gas sensing performance

Yu Hu, Hong Wang, Di Liu, Guo Lin, ... Xiaohua Liu
Pages 5960-5967
View PDF
Article preview

50. ☑ select article High pressure modifications in amorphous boron suboxide: An ab initio study

Research articleAbstract only

High pressure modifications in amorphous boron suboxide: An ab initio study

Murat Durandurdu
Pages 5968-5975
View PDF
Article preview

51. ☑ select article Preparation of oxygen vacancy-controllable CeO₂ by electrotransformation of a CeCl₃ solution and its oxidation mechanism

Research articleAbstract only

Preparation of oxygen vacancy-controllable CeO_2 by electrotransformation of a $CeCl_3$ solution and its oxidation mechanism

Jiang Liu, Zhihe Dou, Ting-an Zhang
Pages 5976-5982
View PDF
Article preview

52. ☑ select article Microstructure evolution in high density AZO ceramic sputtering target fabricated via multistep sintering

Research articleAbstract only

Microstructure evolution in high density AZO ceramic sputtering target fabricated via multistep sintering

Payam Rajabi Kalvani, Samaneh Shapouri, Ali Reza Jahangiri, Yousef Seyed Jalili
Pages 5983-5992
View PDF
Article preview

53. ☑ select article Influence of different coating structures on the oxidation resistance of MoSi₂ coatings

Research articleAbstract only

Influence of different coating structures on the oxidation resistance of $MoSi_2$ coatings

L. Liu, H.Q. Zhang, H. Lei, H.Q. Li, ... C. Sun
Pages 5993-5997
View PDF
Article preview

54. ☑ select article Studying crystal-field splitting difference of Eu³⁺ ions from orthorhombic to cubic Ca₄Al₆SO₁₆

Research articleAbstract only

Studying crystal-field splitting difference of Eu^{3+} ions from orthorhombic to cubic $Ca_4Al_6SO_{16}$

Jinpu Zhang, Jiaming Wu, Xiaolei Lu, Shuwei Ma, ... Xin Cheng
Pages 5998-6005
View PDF
Article preview

55. ☑ select article Electrospun composite nanofibers for intermediate-temperature solid oxide fuel cell electrodes

Research articleAbstract only

Electrospun composite nanofibers for intermediate-temperature solid oxide fuel cell electrodes

Minwoo Ahn, Seungwoo Han, Jongseo Lee, Wonyoung Lee
Pages 6006-6011
View PDF
Article preview

56. ☑ select article Novel direct Z-scheme AgI/N–TiO₂ photocatalyst for removal of polluted tetracycline under visible irradiation

Research articleAbstract only

Novel direct Z-scheme AgI/N–TiO_2 photocatalyst for removal of polluted tetracycline under visible irradiation

Mai Hung Thanh Tung, Nguyen Thi Dieu Cam, Doan Van Thuan, Pham Van Quan, ... Thanh-Dong Pham
Pages 6012-6021
View PDF
Article preview

57. ☑ select article Transformation of metallic polymer precursor into nanosized HfTaC₂ ceramics

Research articleAbstract only

Transformation of metallic polymer precursor into nanosized $HfTaC_2$ ceramics

Yanan Sun, Chunming Yang, Yan Lu, Fenghua Chen, ... Tong Zhao
Pages 6022-6028
View PDF
Article preview

58. ☑ select article A continuum damage mechanics model for 2-D woven oxide/oxide ceramic matrix composites under cyclic thermal shocks

Research articleAbstract only

A continuum damage mechanics model for 2-D woven oxide/oxide ceramic matrix composites under cyclic thermal shocks

Zhengmao Yang, Hui Lui
Pages 6029-6037
View PDF
Article preview

59. ☑ select article Laser surface modification of porous yttria stabilized zirconia against CMAS degradation

Research articleAbstract only

Laser surface modification of porous yttria stabilized zirconia against CMAS degradation

S. Bakkar, M.V. Pantawane, J.J. Gu, A. Ghoshal, ... S.M. Aouadi
Pages 6038-6045
View PDF
Article preview

60. ☑ select article Gamma and neutron shielding characterizations of the Ag₂O–V₂O₅–MoO₃–TeO₂ quaternary tellurite glass system with the Geant4 simulation toolkit and Phy-X software

Research articleAbstract only

Gamma and neutron shielding characterizations of the $Ag_2O–V_2O_5–MoO_3–TeO_2$ quaternary tellurite glass system with the Geant4 simulation toolkit and Phy-X software

A. Aşkın
Pages 6046-6051
View PDF
Article preview

61. ☑ select article Synthesis and morphology optimization of electrospun SiBNC nanofibers

Research articleAbstract only

Synthesis and morphology optimization of electrospun SiBNC nanofibers

Kamal Asadi-Pakdel, Rouhollah Mehdinavaz Aghdam, Mehdi Shahedi Asl, Mohammad Ali Faghihi Sani
Pages 6052-6059
View PDF
Article preview

62. ☑ select article Characterization on the yield stress and interfacial coefficient of friction of glasses from scratch tests

Research articleAbstract only

Characterization on the yield stress and interfacial coefficient of friction of glasses from scratch tests

HaiTao Liu, MingHao Zhao, Chunsheng Lu, JianWei Zhang
Pages 6060-6066

View PDF

Article preview

63. ☑ select article Toward oxygen fully stoichiometric La_{1-x}Sr_xCoO₃ (0.5≤x≤0.9) perovskites: Itinerant magnetic mechanism more than double exchange one's

Research articleAbstract only

Toward oxygen fully stoichiometric $La_{1-x}Sr_xCoO_3$ (0.5≤x≤0.9) perovskites: Itinerant magnetic mechanism more than double exchange one's

Madhu Chennabasappa, Emmauel Petit, Olivier Toulemonde
Pages 6067-6072

View PDF

Article preview

64. ☑ select article Modified structural, optical, magnetic and ferroelectric properties in (1-x) BaTiO₃-xBaCo_{0.5}Nb_{0.5}O_{3-δ} ceramics

Research articleAbstract only

Modified structural, optical, magnetic and ferroelectric properties in $(1-x)BaTiO_3$-$xBaCo_{0.5}Nb_{0.5}O_{3-\delta}$ ceramics

Dongliang Zheng, Hongmei Deng, Shufang Si, Yanlin Pan, ... Junhao Chu
Pages 6073-6078

View PDF

Article preview

65. ☑ select article Novel temperature stable NiSnTa₂O₈ microwave dielectric ceramics with trirutile structure

Research articleAbstract only

Novel temperature stable $NiSnTa_2O_8$ microwave dielectric ceramics with trirutile structure

Enzhu Li, Qingyu Wen, Hongcheng Yang, Hongyu Yang, ... Shuren Zhang
Pages 6079-6084

View PDF

Article preview

66. ☑ select article Synthesis of pyrochlore-borosilicate glass-ceramics for immobilization of high-level nuclear waste

Research articleAbstract only

Synthesis of pyrochlore-borosilicate glass-ceramics for immobilization of high-level nuclear waste

Kangming Wu, Fu Wang, Qilong Liao, Hanzhen Zhu, ... Yongchang Zhu
Pages 6085-6094

View PDF

Article preview

67. ☑ select article Green synthesis of dysprosium stannate nanoparticles using Ficus carica extract as photocatalyst for the degradation of organic pollutants under visible irradiation

Research articleAbstract only

Green synthesis of dysprosium stannate nanoparticles using Ficus carica extract as photocatalyst for the degradation of organic pollutants under visible irradiation

Sahar Zinatloo-Ajabshir, Maryam Sadat Morassaei, Omid Amiri, Masoud Salavati-Niasari
Pages 6095-6107

View PDF

Article preview

68. ☑ select article Crystal structure, relaxor behaviors and energy storage performance of (Sr_{0.7}Ba_{0.3})₅LaNb₇Ti₃O₃₀ tungsten bronze ceramics

Research articleAbstract only

Crystal structure, relaxor behaviors and energy storage performance of $(Sr_{0.7}Ba_{0.3})_5LaNb_7Ti_3O_{30}$ tungsten bronze ceramics

Lei Cao, Ying Yuan, Zhengyi Yang, Enzhu Li, Shuren Zhang
Pages 6108-6114

View PDF

Article preview

69. ☑ select article Ultrasonic-assisted electrodeposition of Ni-Al₂O₃ nanocomposites at various ultrasonic powers

Research articleAbstract only

Ultrasonic-assisted electrodeposition of Ni-Al_2O_3 nanocomposites at various ultrasonic powers

C.Y. Ma, D.Q. Zhao, F.F. Xia, Hanzhao Xia, ... H.Y. Xing
Pages 6115-6123
View PDF
Article preview

70. ☑ select article Evaluation of GO nanosheets decorated by CuFe₂O₄ and CdS nanoparticles as photocatalyst for the degradation of dinoseb and imidacloprid pesticides

Research articleAbstract only

Evaluation of GO nanosheets decorated by $CuFe_2O_4$ and CdS nanoparticles as photocatalyst for the degradation of dinoseb and imidacloprid pesticides

Mostafa Zangiabadi, Asma Saljooqi, Tayebeh Shamspur, Ali Mostafavi
Pages 6124-6128
View PDF
Article preview

71. ☑ select article Design of functionalized α-Fe₂O₃ (III) films with long-term anti-wetting properties

Research articleAbstract only

Design of functionalized α-Fe_2O_3 (III) films with long-term anti-wetting properties

Taotao Liang, Xiaogang Guo, Binfang Yuan, Shuying Kong, ... Xueming Li
Pages 6129-6135
View PDF
Article preview

72. ☑ select article A comprehensive study on the effect of TeO2 on the radiation shielding properties of TeO₂–B₂O₃ –Bi₂O₃–LiF–SrCl₂ glass system using Phy-X / PSD software

Research articleAbstract only

A comprehensive study on the effect of TeO2 on the radiation shielding properties of TeO_2–B_2O_3–Bi_2O_3–LiF–$SrCl_2$ glass system using Phy-X / PSD software

Y. Al-Hadeethi, M.I. Sayyed
Pages 6136-6140
View PDF
Article preview

73. ☑ select article Effect of Nb substitution on magnetic, ferroelectric and photocatalytic properties of Bi_{0.95}Sm_{0.05}Fe_{1-x}Nb_xO₃ (0 ≤ x ≤ 0.1) nanoparticles

Research articleAbstract only

Effect of Nb substitution on magnetic, ferroelectric and photocatalytic properties of $Bi_{0.95}Sm_{0.05}Fe_{1-x}Nb_xO_3$ ($0 \le x \le 0.1$) nanoparticles

F.L. Wang, Y. Li, N. Wang, Aditya Jain, ... F.G. Chen
Pages 6141-6145
View PDF
Article preview

74. ☑ select article Preparation of spherical and porous strontium titanate particles by hot water and hydrothermal conversion of hydrous titania

Research articleAbstract only

Preparation of spherical and porous strontium titanate particles by hot water and hydrothermal conversion of hydrous titania

Kazuya Ujiie, Takashi Kojima, Kosuke Ota, Pornjira Phuenhinlad, ... Naofumi Uekawa
Pages 6146-6153
View PDF
Article preview

75. ☑ select article Luminescence and self-referenced optical temperature sensing performance in Ca₂YZr₂Al₃O₁₂:Bi³⁺,Eu³⁺ phosphors

Research articleAbstract only

Luminescence and self-referenced optical temperature sensing performance in $Ca_2YZr_2Al_3O_{12}:Bi^{3+},Eu^{3+}$ phosphors

Zhigang Zheng, Jiafei Zhang, Xueyun Liu, Rongfei Wei, ... Hai Guo
Pages 6154-6159
View PDF
Article preview

76. ☑ select article Phase relations in the “FeO–V₂O₃” system at 1473 K and the magnetic properties of spinel phase Fe_{3-x}V_xO₄

Research articleAbstract only

Phase relations in the “$FeO–V_2O_3$” system at 1473 K and the magnetic properties of spinel phase $Fe_{3-x}V_xO_4$

Baijun Yan, Daya Wang, Qiugen Qiu, Tengfei Deng
Pages 6160-6167
View PDF
Article preview

77. ☑ select article High temperature microwave absorbing properties of plasma sprayed La_{0.6}Sr_{0.4}FeO₃-_δ/MgAl₂O₄ composite ceramic coatings

Research articleAbstract only

High temperature microwave absorbing properties of plasma sprayed $La_{0.6}Sr_{0.4}FeO_{3-\delta}/MgAl_2O_4$ composite ceramic coatings

Hongyao Jia, Wancheng Zhou, Hanyi Nan, Yuchang Qing, ... Dongmei Zhu
Pages 6168-6173
View PDF
Article preview

78. ☑ select article Impact of ZrO₂ alloying on thermo-mechanical properties of Gd₃NbO₇

Research articleAbstract only

Impact of ZrO_2 alloying on thermo-mechanical properties of Gd_3NbO_7

YiTao Wang, Lin Chen, Jing Feng
Pages 6174-6181
View PDF
Article preview

79. ☑ select article Effect of additives on slip casting rheology, microstructure and mechanical properties of Si₃N₄/SiC composites

Research articleAbstract only

Effect of additives on slip casting rheology, microstructure and mechanical properties of Si_3N_4/SiC composites

Shohreh Shahrestani, Mokhtar Che Ismail, Saeid Kakooei, Mohammadali Beheshti
Pages 6182-6190
View PDF
Article preview

80. ☑ select article Composite fibers of La_{0.5}Sr_{0.5}CoO_{3-δ}-LaSrCoO_{4±δ} with high catalytic activity toward oxygen reduction reaction

Research articleAbstract only

Composite fibers of $La_{0.5}Sr_{0.5}CoO_{3-\delta}$-$LaSrCoO_{4\pm\delta}$ with high catalytic activity toward oxygen reduction reaction

Fushao Li, Yingxian Xu, Feixiang Cheng, Yuxing Yan, ... Long Jiang
Pages 6191-6198
View PDF
Article preview

81. ☑ select article 2D Ti₃C₂T_x MXene/aramid nanofibers composite films prepared via a simple filtration method with excellent mechanical and electromagnetic interference shielding properties

Research articleAbstract only

2D $Ti_3C_2T_x$ MXene/aramid nanofibers composite films prepared via a simple filtration method with excellent mechanical and electromagnetic interference shielding properties

Huawei Wei, Mingqiang Wang, Wenhui Zheng, Zaixing Jiang, Yudong Huang
Pages 6199-6204
View PDF

Article preview

82. ☑ select article Effect of varying Al₂O₃ contents of CaO–Al₂O₃–SiO₂ slags on lumped MgO dissolution

Research articleAbstract only

Effect of varying Al_2O_3 contents of CaO–Al_2O_3–SiO_2 slags on lumped MgO dissolution

Yelim Kim, Yoshiaki Kashiwaya, Yongsug Chung
Pages 6205-6211
View PDF
Article preview

83. ☑ select article A novel piezoelectric ceramic with high Curie temperature and high piezoelectric coefficient

Research articleAbstract only

A novel piezoelectric ceramic with high Curie temperature and high piezoelectric coefficient

Siyu Huang, Jiangtao Zeng, Liaoying Zheng, Zhenyong Man, ... Guorong Li
Pages 6212-6216
View PDF
Article preview

84. ☑ select article Synthesis of LiBaZrO_x ceramics with a core-shell structure

Research articleAbstract only

Synthesis of $LiBaZrO_x$ ceramics with a core-shell structure

M.V. Zdorovets, A. Arbuz, A.L. Kozlovskiy
Pages 6217-6221
View PDF
Article preview

85. ☑ select article Hydrothermal synthesis and characterization studies of α-Fe₂O₃/MnO₂ nanocomposites for energy storage supercapacitor application

Research articleAbstract only

Hydrothermal synthesis and characterization studies of α-Fe_2O_3/MnO_2 nanocomposites for energy storage supercapacitor application

Mohamed Racik K, A. Manikandan, M. Mahendiran, J. Madhavan, ... T. Maiyalagan
Pages 6222-6233
View PDF
Article preview

86. ☑ select article 3D-SiC decorated with SiC whiskers: Chemical vapor infiltration on the porous 3D-SiC lattices derived from polycarbosilane-based suspensions

Research articleAbstract only

3D-SiC decorated with SiC whiskers: Chemical vapor infiltration on the porous 3D-SiC lattices derived from polycarbosilane-based suspensions

Huiwen Xiong, Hehao Chen, Zhaoke Chen, Xiang Xiong, ... Kechao Zhou
Pages 6234-6242
View PDF
Article preview

87. ☑ select article Nanomechanical characterization of RB-SiC ceramics based on nanoindentation and modelling of the ground surface roughness

Research articleAbstract only

Nanomechanical characterization of RB-SiC ceramics based on nanoindentation and modelling of the ground surface roughness

Zhenzhong Zhang, Peng Yao, Jun Wang, Chuanzhen Huang, ... Bin Zou
Pages 6243-6253
View PDF
Article preview

88. ☑ select article Oxidation and cracking/spallation resistance of ZrB₂–SiC–TaSi₂–Si coating on siliconized graphite at 1500 °C in air

Research articleAbstract only

Oxidation and cracking/spallation resistance of ZrB_2–SiC–$TaSi_2$–Si coating on siliconized graphite at 1500 °C in air

Yan Ren, Yuhai Qian, Jingjun Xu, Yan Jiang, ... Meishuan Li
Pages 6254-6261
View PDF
Article preview

89. ☑ select article Robust assembly of urchin-like NiCo₂O₄/CNTs architecture as bifunctional electrocatalyst in Zn-Air batteries

Research articleAbstract only

Robust assembly of urchin-like $NiCo_2O_4$/CNTs architecture as bifunctional electrocatalyst in Zn-Air batteries

Xiao Xiao, Xinhai Li, Jiexi Wang, Guochun Yan, ... Yong Liu
Pages 6262-6269
View PDF
Article preview

90. ☑ select article Thermo-mechanical behaviours of Li_{3x}La_{1/3-x}MO₃ (M = Ta and Nb)

Research articleAbstract only

Thermo-mechanical behaviours of $Li_{3x}La_{1/3-x}MO_3$ (M = Ta and Nb)

Wakako Araki, Yasuhiro Nagakura, Yoshio Arai
Pages 6270-6275
View PDF
Article preview

91. ☑ select article Synthesis, energy transfer mechanism, and tunable emissions of novel Na₃La(VO₄)₂:Re³⁺ (Re³⁺ = Dy³⁺, Eu³⁺, and Sm³⁺) vanadate phosphors for near-UV-excited white LEDs

Research articleAbstract only

Synthesis, energy transfer mechanism, and tunable emissions of novel $Na_3La(VO_4)_2$:Re^{3+} (Re^{3+} = Dy^{3+}, Eu^{3+}, and Sm^{3+}) vanadate phosphors for near-UV-excited white LEDs

Jiangcong Zhou, Yao Yao, Yu Chen, Bo Wang, ... Quansheng Wu
Pages 6276-6283
View PDF
Article preview

92. ☑ select article Photocatalytic activity of copper ferrite graphene oxide particles for an efficient catalytic degradation of Reactive Black 5 in water

Research articleAbstract only

Photocatalytic activity of copper ferrite graphene oxide particles for an efficient catalytic degradation of Reactive Black 5 in water

Rasmus Kodasma, Burcu Palas, Gülin Ersöz, Süheyda Atalay
Pages 6284-6292
View PDF
Article preview

93. ☑ select article Anomalous thermal expansion behavior in Er_{1-x}Ca_xMnO₃

Research articleAbstract only

Anomalous thermal expansion behavior in $Er_{1-x}Ca_xMnO_3$

Yajie Jiao, Hui Wang, Mengjie Yang, Mingju Chao, ... Erjun Liang
Pages 6293-6299
View PDF
Article preview

94. ☑ select article Ti(C,N)-based cermets with fine grains and uniformly dispersed binders: Effect of the Ni–Co based binders

Research articleAbstract only

Ti(C,N)-based cermets with fine grains and uniformly dispersed binders: Effect of the Ni–Co based binders

Dingqian Dong, Wei Yang, Huiwen Xiong, Li Zhang, ... Jun Liao
Pages 6300-6310
View PDF

Article preview

95. ☑ select article Characteristics of Optimized Al:ZnO sputtering targets prepared by nanostructured powder

Research articleAbstract only

Characteristics of Optimized Al:ZnO sputtering targets prepared by nanostructured powder

Haichao Liu, Ming Gao, Benrun Yang, Haojie Chen, ... Hu Zhang
Pages 6311-6317
View PDF
Article preview

96. ☑ select article Optical, structural, morphological, and compositional properties of cobalt doped tin oxide (CTO) thin films deposited by modified chemical bath method in alkaline medium

Research articleAbstract only

Optical, structural, morphological, and compositional properties of cobalt doped tin oxide (CTO) thin films deposited by modified chemical bath method in alkaline medium

L.N. Ezenwaka, N.S. Umeokwonna, N.L. Okoli
Pages 6318-6325
View PDF
Article preview

97. ☑ select article Preparation and characterization of organic-inorganic hybrid ZrOC/PF aerogel used as high-temperature insulator

Research articleAbstract only

Preparation and characterization of organic-inorganic hybrid ZrOC/PF aerogel used as high-temperature insulator

Sue Ren, li Hu, Xiutao Li, Jinpeng Fan, Jun Liang
Pages 6326-6332
View PDF
Article preview

Previous page 1 of 2 Next

Previous vol/issue

Next vol/issue

ISSN: 0272-8842

Ceramics International 46 (2020) 5850–5855

Contents lists available at ScienceDirect

Ceramics International

journal homepage: www.elsevier.com/locate/ceramint

Size controlled synthesis of well-distributed nano-silver on hydroxyapatite using alkanolamine compounds

Arniati Labanni[a], Zulhadjri[a], Dian Handayani[b], Yutaka Ohya[c], Syukri Arief[a,*]

[a] Department of Chemistry, Faculty of Mathematics and Sciences, Andalas University, Padang, 25163, Indonesia
[b] Faculty of Pharmacy, Andalas University, Padang, 25163, Indonesia
[c] Department of Chemistry and Biomolecular Science, Faculty of Engineering, Gifu University, Yanagido 1 – 1, Gifu, 501-1193, Japan

ARTICLE INFO

Keywords:
Silver nanoparticle
Silver hydroxyapatite composite
Uncaria gambir Roxb.
Bone implant

ABSTRACT

A well-distributed nano-silver hydroxyapatite composite has been successfully prepared by a one-pot synthesis method. Hydroxyapatite was separately synthesized by a sol-gel method, then impregnated with silver nanoparticles with the mediation of *Uncaria gambir* Roxb. leaf extract in the presence of three kinds of alkanolamine compound; monoethanolamine (MEA), diethanolamine (DEA), and triethanolamine (TEA) as capping agents. The effect of different capping agents on the properties of the silver nanoparticles and the nano-silver hydroxyapatite composite were studied. UV–visible spectrophotometer analysis exhibited absorbance peaks at 402–439 nm which specifically corresponds to spherical silver nanoparticles. Higher optical absorbance was observed in TEA-capped silver nanoparticles, than in DEA and MEA-capped ones. X-ray diffraction (XRD) analysis showed a highly crystalline hexagonal structure for hydroxyapatite and no detected metallic silver. However, the presence of 1.65% silver was confirmed by energy dispersive x-ray (EDX) spectroscopy analysis. Transmission electron microscopy (TEM) analysis revealed spherical silver nanoparticles with a size range of 2–62 nm (smallest mean diameter of 2 nm) adhered to the hydroxyapatite surface. The TEA capped impregnated silver nanoparticles were the smallest, corresponding to the best capping performance, followed by those capped by DEA and MEA. Small-sized nanoparticles on hydroxyapatite are beneficial for highly antibacterial bone implants.

1. Introduction

In recent decades, the study of calcium orthophosphate based inorganic biomaterials has been of increasing interest due to their wide applications in the field of health and medicine [1–3]. One of the most studied of these is hydroxyapatite (HA) (chemical formula $Ca_{10}(PO_4)_6(OH)_2$) which is used as a graft material for bone and for tooth substitution and repair due to its biocompatibility, bioactivity, and osteoconductivity [4,5]. Synthesis of hydroxyapatite has been achieved using a hydrothermal method [6], a microwave-assisted method [1], sol-gel [2], and a precipitation method [5]. The sol-gel method is considered efficient, easy, and environmentally friendly as it is low-cost, requires a low formation temperature and yet achieves high degrees of homogeneity and purity [7].

However, one of the main problems of this material is infections that can occur after bone implantation or other surgical operations since these biomaterials provide sites for potential bacteria adhesion. This process might be due to the absorption of protein, amino acid, and any other organic compounds into HA [8]. Furthermore, antibiotics loaded into implant material tend to be rapidly flushed out by body flood resulting in long term post-surgical infections [9]. This situation is made worse by the increase of multi-drug resistant (MDR) bacteria. Therefore, there is a demand for the development of a new generation of modified antibacterial agents to solve this problem [10,11]. Nanotechnology offers a promising approach to the fabrication of antibacterial agents in the form of metallic nanoparticles. In recent years, silver nanoparticles with their antibacterial properties have gained a lot of attention due to their potential applications in the biomedical field [12,13]. It could be expected that the incorporation of silver nanoparticles into hydroxyapatite could help avoid post-operative inflammation and bacterial infection [14]. In addition, compared to bulk materials, silver nanoparticles have excellent properties due to the high surface area to volume ratio which results in a beneficial effect at low concentrations when incorporated into a biomaterial. This point is crucial for the health of the patient as it minimizes the amount of this metal in the body [15].

* Corresponding author.
E-mail address: syukriarief@sci.unand.ac.id (S. Arief).

https://doi.org/10.1016/j.ceramint.2019.11.035
Received 16 August 2019; Received in revised form 4 November 2019; Accepted 5 November 2019
Available online 06 November 2019

In our previous studies, stable colloidal silver nanoparticles have been successfully synthesized by bio-reducing Ag^+ using *Uncaria gambir* Roxb. as a reducing agent in presence of MEA [16] and DEA [17] as a capping agent. *Uncaria gambir* Roxb. is one of commodity in West Sumatera, Indonesia and for long time had been used as traditional medicine due to the content of some polyphenol compounds predominantly catechin. Those polyphenol compound is expected to reduce Ag^+ to Ag^0. The formation of those stable and small-sized colloidal silver nanoparticles was conducted using a simple method and did not require the use of expensive technological equipment. Modifying this method of silver nanoparticle fabrication by the addition of a capping agent should result in control over their size and stability which would be advantageous since the antibacterial activity of metallic nanoparticles is strongly influenced by size [18]. Hence, in this study, three kinds of alkanolamine compound, i.e. MEA, DEA, and TEA were trialled as capping agents in the preparation of silver nanoparticles using *Uncaria gambir* Roxb. leaf extract using 1 pot synthesis with hydroxyapatite powder. The effect of alkanolamine compound structure on the properties of silver nanoparticles was studied and the effect of each capping agent were compared using UV–Vis spectrophotometry, XRD, EDX, and TEM analysis.

2. Experimental procedures

2.1. Synthesis of hydroxyapatite

Hydroxyapatite was separately synthesized using a sol-gel method based on previous report by Jamarun et al. [7]. The calcium precursor used in the reaction was extracted from cockle shells (*Anadara granosa)* as in Azis et al. (2015) [6]. The cockle shells were cleaned, washed, dried, and ground to a coarse powder. They were then calcined at 900 °C for 5 h to obtain CaO. $(NH_4)_2HPO_4$ (Merck, analytical grade) was used as a phosphor precursor.

This CaO was diluted into HNO_3 2 M (Merck, analytical grade) and then stirred at a constant rate of 600 rpm at 85 °C for 20 min 250 ml $(NH_4)_2HPO_4$ was added drop-wise to the solution while stirring at 110 °C and pH adjusted to 11 using NH_4OH (Merck, Analytical grade). The mixture was stirred for 5 h to obtain white sol. After 24 h of aging, the gel was filtered and dried in a 110 °C oven for 6 h to obtain a powder. This was then calcined at 900 °C for 5 h resulting in hydroxyapatite.

2.2. Synthesis of HAp-AgNps composite

Uncaria gambir Roxb. leaves were taken from the experimental garden, Andalas University, Padang, Indonesia and extracted using the method of Labanni et al. [16]. Fresh leaves were washed, dehydrated by shade drying, and mashed up to obtain powder. Extraction was conducted using water solvent and stirring at a constant rate at 65 °C for 2 h then filtered. This filtrate was then stored in a sealed bottle at 4 °C.

Nano-silver hydroxyapatite composite was fabricated by precipitation method. 1 mM silver nitrate (Merck, Analytical grade), 2 mM of the chosen alkanolamine (Merck, Analytical grade), and 4% leaf extract with as-synthesized hydroxyapatite to make a total volume of 50 mL were stirred together in a dark environment in 1 pot for 24 h at a constant rate of 600 rpm at room temperature. After stirring, the mixture was filtered and the residue was washed using distilled water, then dried in a hot air oven to produce powder. The synthesized nano-silver hydroxyapatite composite fabricated using MEA, DEA, or TEA as a capping agent are hereafter denoted as HAp-AgNps MEA, HAp-AgNps DEA, and HAp-AgNps TEA, respectively. In addition, the synthesis of HAp-AgNps without the use of a capping agent was also carried out as control, which is hereafter denoted as HAp-AgNps0.

2.3. Characterization

The UV–Vis Spectrophotometry analysis of silver nanoparticles was carried out using Thermo Scientific Evolution 201 UV–Vis in wavelength range of 200–800 nm. The crystal structure of synthesized HAp-AgNps was investigated using X-Ray Diffraction Rigaku Ultima IV with CuKα radiation with a scanning rate of 2° min^{-1} at 60 kV and 20 mA. The size and the morphology of HAp-AgNps were evaluated using JEOL JEM 2100. Chemical composition of the samples was determined using EDX JEOL JED 2300.

3. Results and discussion

3.1. UV–Vis Spectrophotometry analysis

The formation of silver nanoparticles was indicated by a colour change from colourless to yellowish-brown 5 min after the reaction. The presence of the particles was then tested by UV–Vis spectrophotometry analysis over the wavelength range of 200–800 nm (Fig. 1). Optical absorption peaks occurring at 402–439 nm were observed in all four samples. The absorbance value increased with the presence of alkanolamine in the reaction which suggested that, besides acting as a capping agent as expected, these alkanolamine compounds acted as reducing agents as well. AgNps-TEA provided the highest absorbance value followed by AgNps-DEA, then AgNps-MEA. This result suggested that the structure of alkanolamine compounds used significantly affects the number of silver nanoparticles formed in the reaction. This might be due to the number of hydroxyl groups in the structure, which have a role in reducing silver cations to metallic silver. Furthermore, the use of different alkanolamine compounds also resulted in different wavelength ranges in the absorbance spectrum, with AgNps-TEA absorbing at shorter wavelength than AgNps-DEA and AgNps-MEA. The Mie theory of scattering for spherical metal nanoparticles indicates that a shift to longer wavelength corresponds to a larger particle size [19]. Hence, this result suggests that the use of TEA resulted in smaller sized nanoparticles than those of DEA and MEA capped reactions. AgNps-TEA capped nanoparticles also had a narrower absorbance peak suggesting a narrower size range. This result was subsequently affirmed by TEM analysis.

3.2. X-ray diffraction analysis

The result of XRD analysis of the HAp-AgNps powder synthesized with each alkanolamine compound is displayed in Fig. 2. The diffraction pattern of HAp-AgNps in all samples showed peaks at 2θ values of 26.10, 32.00, 32.43, 33.16, 46.86, and 49.62° indicating a well-

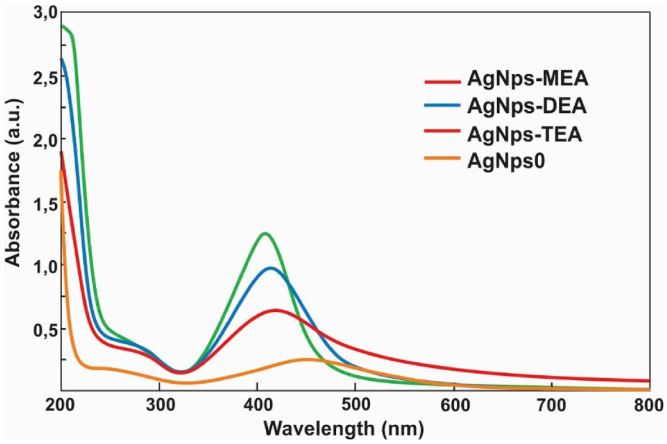

Fig. 1. UV–Vis absorption spectrum of *Uncaria gambir* Roxb. mediated silver nanoparticle with alkanolamine compounds as capping agent.

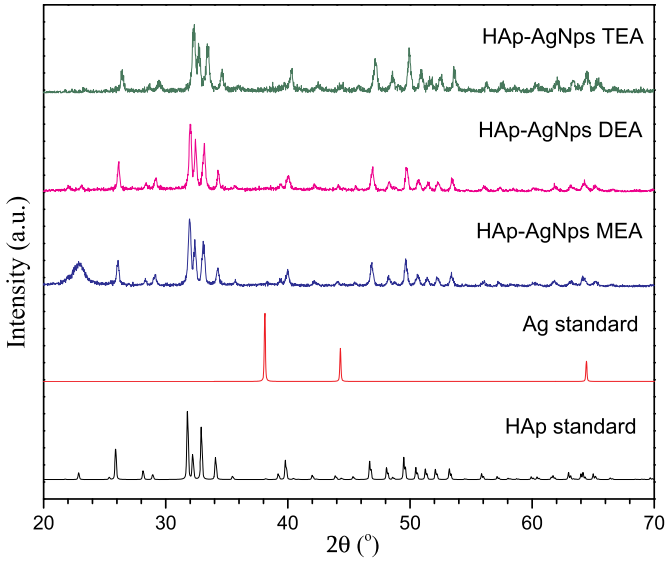

Fig. 2. XRD pattern of synthesized HAp-AgNps.

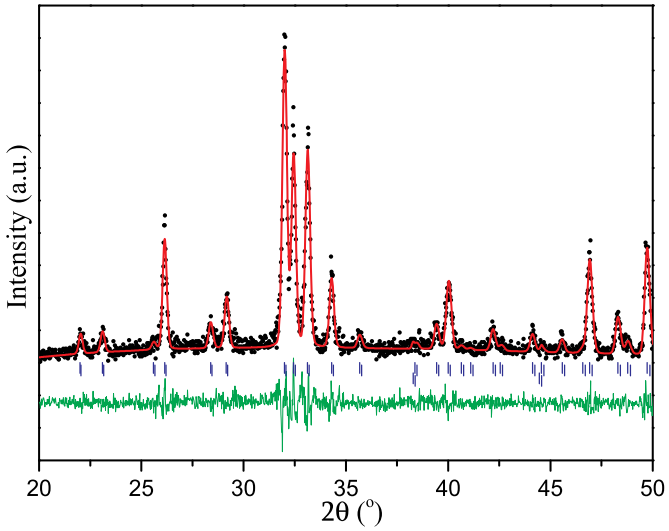

Fig. 3. XRD pattern fitted with Le Bail method for bi-phasic HAp-AgNps.

crystallized hexagonal structured hydroxyapatite based on the ICSD #26204 standard. This result indicated that hydroxyapatite had been successfully synthesized using *Anadara granosa* as a calcium precursor using sol-gel method. The metallic silver was not evident in the diffraction pattern of the HAp-AgNps samples. Similar results have also been found in previous researches about HAp-AgNps composite, where metallic silver was not detected in XRD analysis [20,21]. In fact, the percentage of silver nanoparticles was very small compared to hydroxyapatite in the samples and this could be the reason for the lack of observable metallic silver peaks.

In order to display the metallic silver peak in XRD analysis more clearly, Le Bail refinement was conducted on one of the samples using Rietica software using 2 phase standards of hydroxyapatite and silver. The plot is shown in Fig. 3, where the black circles represent the experimental XRD data, the red line represents calculated data of both hexagonal hydroxyapatite and face-centred cubic silver phases, and the green line represents the difference pattern. The result shows the presence of Ag at 2θ of 38.20 and 44.21°, marked by an asterisk (*), in accordance with the ICSD #604631 standard for metallic silver. The Rp value was found to be 16.09 with a goodness of fit (χ^2) of 2.169 which is an acceptable value according to the basic principles of goodness of fit [22]. In comparison to this result, the Rp value of single-phase hydroxyapatite refinement was found to be 16.72. The decrease of the Rp value in two-phase refinement indicates the presence of the Ag peak in the diffraction pattern.

3.3. Energy dispersive X-Ray analysis

Elemental analysis using EDX further confirmed the presence of Ag in the samples. Fig. 4 showed the elemental analysis result of HAp-AgNps TEA with an Ag peak at approximately 3 keV, with a mass percentage of 1.68%. This clearly confirmed the presence of silver in the samples as indicated in the XRD analysis. Not surprisingly, Ca and P were also evident in the sample from the content of the hydroxyapatite.

3.4. Transmission electron microscopy analysis

The presence of nanometer-sized silver was clearly observed in the TEM. Spherical nanoparticles with size range of 2–15 nm could be clearly observed attached on the surface of micrometer-sized hydroxyapatite (Fig. 5). The very small size and ratio of silver nanoparticle compared to hydroxyapatite is a strong reason for the absence of metallic silver peaks in the XRD analysis result. A highly significant difference was observed between the appearance of the capped HAp-

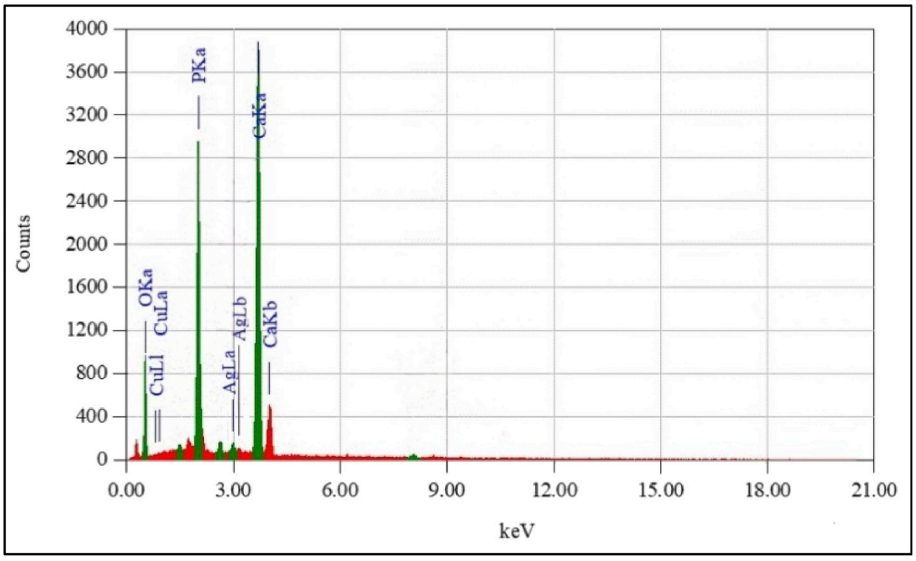

Fig. 4. EDX analysis of HAp-AgNps TEA.

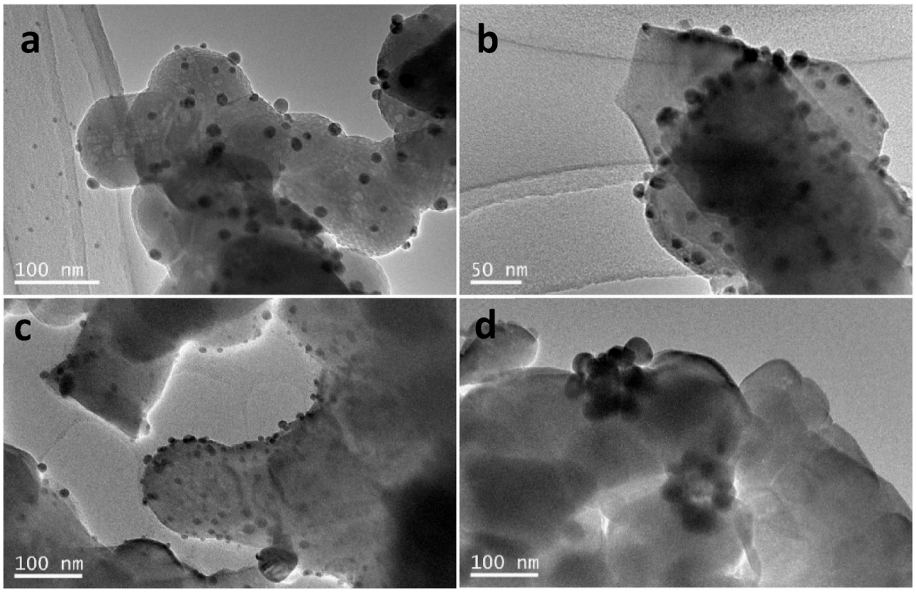

Fig. 5. TEM Images of a) HAp-AgNps MEA, b) HAp-AgNps DEA, c) HAp-AgNps TEA, and d) HAp-AgNps0.

AgNps and AgNps0. Silver nanoparticles on HAp-AgNps0 (Fig. 5d) tended to be stacked and agglomerated in certain sites, while in HAp AgNps-MEA, HAp-AgNps DEA, and HAp-AgNps TEA (Fig. 5a, b, c) silver nanoparticles were well distributed over the HAp surface. A similar result has been previously reported by Nirmala et al. [23] who synthesized HAp-AgNps from bovine femur bone where hydroxyapatite was presented as microstructure with silver nanoparticles attached on the periphery. The present results clearly suggest that the use of

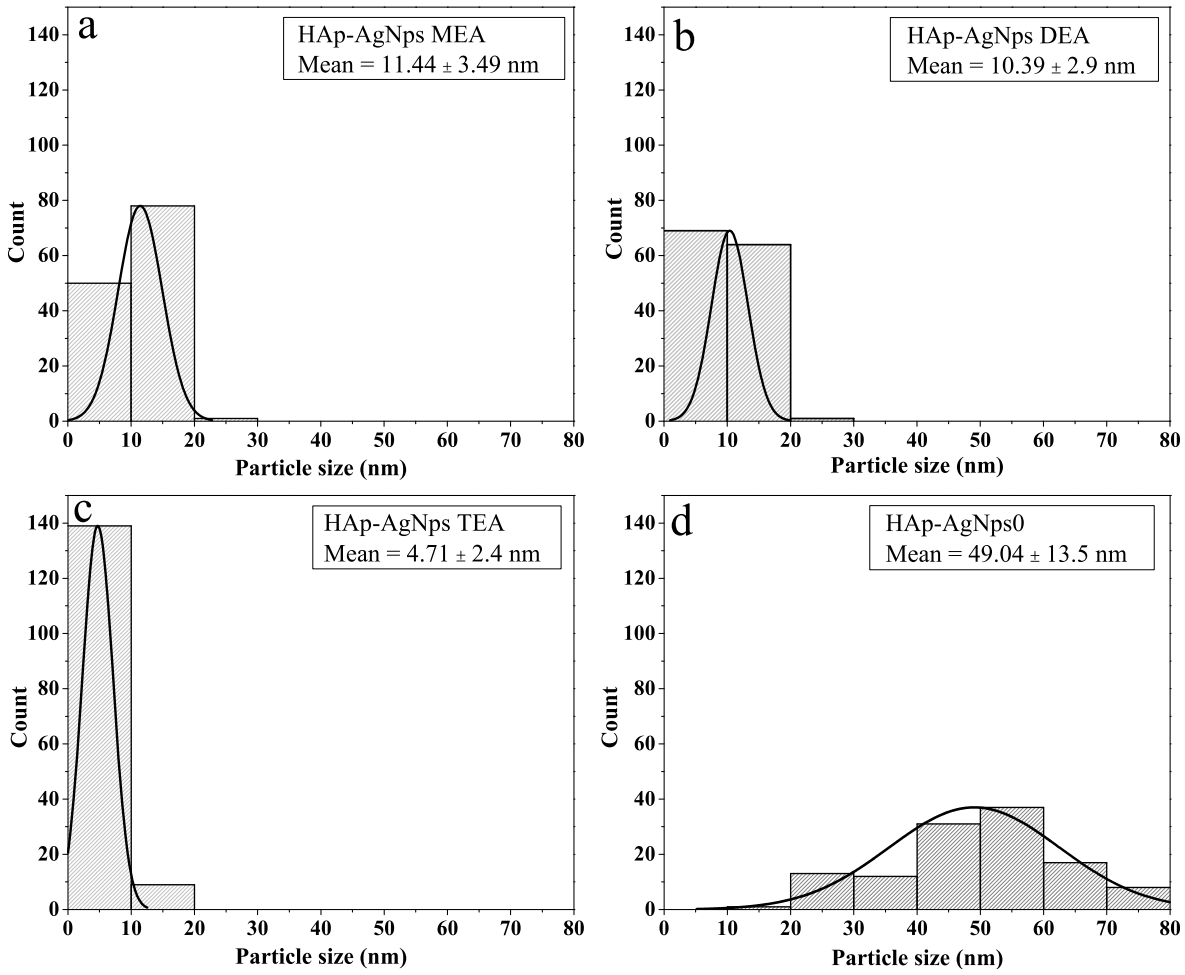

Fig. 6. Particle size distribution of AgNps on a) HAp-AgNps MEA, b) HAp-AgNps DEA, c) HAp-AgNps TEA, and d) HAp-AgNps0.

alkanolamine compounds strongly affects the distribution of AgNps on the HAp surface. The attachment of silver nanoparticles on the surface of an implant is more advantageous for antibacterial activity than silver nanoparticles attached inside the implant [24].

Fig. 6 shows particle size distribution of as-synthesized HAp-AgNps as determined by ImageJ software. It was discovered that the mean diameter of nano-silver in HAp-AgNps0 was 49 nm, 10 times larger than that of nano-silver in HAp-AgNps TEA. In addition, nano-silver in HAp-AgNps0 (Fig. 6d) showed a much broader particle size range than those in the alkanolamine capped samples indicating that the use of capping agents was indeed able to control growth and affect the size uniformity of nanoparticles.

In addition, there was a correlation between the type of capping agent used (MEA, DEA, and TEA) and the size of silver nanoparticles. Nano-silver in HAp-AgNps TEA provided the smallest particle size, followed by nano-silver in HAp-AgNps DEA, then HAp-AgNps MEA. As TEA has more hydroxyl groups than DEA and MEA has even fewer, it is concluded that the higher number of hydroxyl groups in the structure results in the smaller mean size. Several studies have reported that in the stabilizing mechanism of silver nanoparticles by alkanolamine compounds, an electrostatic interaction occurs between free electron pairs from nitrogen and positively charged AgNps, resulting in a protective monolayer. This monolayer then caps nanoparticles to avoid excessive fusion, hence controls the growth and size of nanoparticles [16,25,26]. It is assumed that hydroxyl groups of alkanolamine compound obstruct further interaction among silver nanoparticles. The higher number of hydroxyl groups in TEA could be the reason for the optimum capping performance of TEA, thus resulting in the smallest nanoparticle size seen in the TEM as well as the wavelength shift in the UV–Vis spectrophotometry analysis. These silver nanoparticles are of a much smaller size than those previously reported by Bharti et al. who used trisodium citrate as a reducing agent, resulting in nano-silver with mean particle size of 58.38 nm [27].

4. Conclusion

A well-distributed nano-silver hydroxyapatite composite has been successfully synthesized using a 1 pot green synthesis method with *Uncaria gambir* Roxb. leaf extract as the bio-reducing agent and each of three different alkanolamine compounds as capping agents. UV–Vis spectrophotometry and EDX analysis confirmed the formation of silver nanoparticles. XRD analysis showed the formation of a highly crystalline hexagonal structured hydroxyapatite. TEM analysis confirmed the presence of spherical silver nanoparticles with a diameter range of 2–62 nm adhering to the hydroxyapatite surface. The results suggested that alkanolamine compounds can play a crucial role in fabricating stable and well-distributed silver nanoparticles on the hydroxyapatite surface. HAp-AgNps TEA showed smaller AgNps than those of MEA and DEA. This small size indicates that although the amount of silver contained in the hydroxyapatite compound was extremely small, the silver's surface distribution should have a significant antibacterial impact. Silver nanoparticles incorporated hydroxyapatite using Uncaria gambir Roxb. leaf extract and TEA could produce materials highly suitable for biomedical applications.

Declaration of competing interest

The authors declare that they have no known competing financial interests or personal relationships that could have appeared to influence the work reported in this paper.

Acknowledgement

The authors would like to thank the Ministry of Research, Technology and Higher Education of the Republic of Indonesia and LPPM of Andalas University for funding this work through the research grants of PMDSU programme and PKPI PMDSU 2018.

References

[1] S. Türk, Altınsoy, G. ÇelebiEfe, M. Ipek, M. Özacar, C. Bindal, Microwave–assisted biomimetic synthesis of hydroxyapatite using different sources of calcium, Mater. Sci. Eng. C 76 (2017) 528–535, https://doi.org/10.1016/j.msec.2017.03.116.
[2] I. Bogdanoviciene, K. Tonsuaadu, V. Mikli, I. Grigoraviciute-Puroniene, A. Beganskiene, A. Kareiva, pH impact on the sol-gel preparation of calcium hydroxyapatite, Ca10(PO4)6(OH)2, using a novel complexing agent, DCTA, Cent. Eur. J. Chem. 8 (2010) 1323–1330, https://doi.org/10.2478/s11532-010-0113-0.
[3] N. Jamarun, Z. Azharman, S. Arief, T.P. Sari, A. Asril, S. Elfina, Effect of temperature on synthesis of hydroxyapatite from limestone, Rasayan J. Chem. 8 (2015) 133–137.
[4] A. Szcześ, L. Hołysz, E. Chibowski, Synthesis of hydroxyapatite for biomedical applications, Adv. Colloid Interface Sci. 249 (2017) 321–330, https://doi.org/10.1016/j.cis.2017.04.007.
[5] B. Cengiz, Y. Gokce, N. Yildiz, Z. Aktas, A. Calimli, Synthesis and characterization of hydroxyapatite nanoparticles, Colloid. Surf. Physicochem. Eng. Asp 322 (2008) 29–33, https://doi.org/10.1016/j.colsurfa.2008.02.011.
[6] Y. Azis, N. Jamarun, S. Arief, H. Nur, Facile synthesis of hydroxyapatite particles from cockle shells (Anadara granosa) by hydrothermal method, Orient, J. Chem. 31 (2015) 1099–1105, https://doi.org/10.13005/ojc/310261.
[7] N. Jamarun, Miftahurrahmi, U. Septiani, Synthesis of hydroxyapatite from halaban limestone by sol-gel method, Res. J. Pharm. Biol. Chem. Sci. 7 (2016) 2956–2961.
[8] S. Jadalannagari, K. Deshmukh, S.R. Ramanan, M. Kowshik, Antimicrobial activity of hemocompatible silver doped hydroxyapatite nanoparticles synthesized by modified sol–gel technique, Appl. Nanosci. 4 (2014) 133–141, https://doi.org/10.1007/s13204-013-0197-x.
[9] V. Stanić, D. Janaćković, S. Dimitrijević, S.B. Tanasković, M. Mitrić, M.S. Pavlović, A. Krstić, D. Jovanović, S. Raičević, Synthesis of antimicrobial monophase silver-doped hydroxyapatite nanopowders for bone tissue engineering, Appl. Surf. Sci. 257 (2011) 4510–4518, https://doi.org/10.1016/j.apsusc.2010.12.113.
[10] A. Akhavan, N. Sheikh, F. Khoylou, F. Naimian, E. Ataeivarjovi, Synthesis of antimicrobial silver/hydroxyapatite nanocomposite by gamma irradiation, Radiat. Phys. Chem. 98 (2014) 46–50, https://doi.org/10.1016/j.radphyschem.2014.01.004.
[11] A. Bharti, S. Singh, V.K. Meena, N. Goyal, Synthesis of novel multiple shaped silver nanoparticles incorporated hydroxyapatite nanocomposite for orthopaedic body implants, Adv. Sci. Lett. 20 (2014) 1297–1302, https://doi.org/10.1166/asl.2014.5508.
[12] H. Nikaido, Multidrug resistance in bacteria, Annu. Rev. Biochem. 78 (2009) 119–146, https://doi.org/10.1146/annurev.biochem.78.082907.145923.Multidrug.
[13] M.K. Rai, S. Deshmukh, A. Ingle, A.K. Gade, Silver nanoparticles: the powerful nanoweapon against multidrug-resistant bacteria, J. Appl. Microbiol. 112 (2012) 841–852, https://doi.org/10.1111/j.1365-2672.2012.05253.x.
[14] A. Mocanu, G. Furtos, S. Rapuntean, O. Horovitz, C. Flore, C. Garbo, A. Danisteanu, G. Rapuntean, C. Prejmerean, M. Tomoaia-Cotisel, Synthesis; characterization and antimicrobial effects of composites based on multi-substituted hydroxyapatite and silver nanoparticles, Appl. Surf. Sci. 298 (2014) 225–235, https://doi.org/10.1016/j.apsusc.2014.01.166.
[15] N.A. Charlena, Handika Nuzulia, Synthesis and characterization of composite synthesis and characterization of composite hydroxyapatite-silver nanoparticles, IOP Conf. Ser. Earth Environ. Sci. 58 (2017) 1, https://doi.org/10.1088/1755-1315/5.
[16] A. Labanni, Z. Zulhadjri, D. Handayani, Y. Ohya, The effect of monoethanolamine as stabilizing agent in Uncaria gambir Roxb . mediated synthesis of silver nanoparticles and its antibacterial activity, J. Dispersion Sci. Technol. (2019) 1–8, https://doi.org/10.1080/01932691.2019.1626249.
[17] A. Labanni, Zulhadjri, D. Handayani, S. Arief, Uncaria gambir Roxb. mediated green synthesis of silver nanoparticles using diethanolamine as capping agent, IOP Conf. Ser. Mater. Sci. Eng, 2018, pp. 1–6, , https://doi.org/10.1088/1757-899X/299/1/012067.
[18] N. Jafari, L. Karimi, M. Mirjalili, S.J. Derakhshan, Effect of Silver Particle size on color and Antibacterial properties of silk and cotton Fabrics, Fibers Polym. 17 (2016) 888–895, https://doi.org/10.1007/s12221-016-6052-4.
[19] M. Guzman, J. Dille, S. Godet, Synthesis and antibacterial activity of silver nanoparticles against gram-positive and gram-negative bacteria, Nanomed. Nanotechnol. Biol. Med. 8 (2012) 37–45, https://doi.org/10.1016/j.nano.2011.05.007.
[20] F.A.C. Andrade, L.C.D.O. Vercik, F.J. Monteiro, E.C.D.S. Rigo, Preparation, characterization and antibacterial properties of silver nanoparticles-hydroxyapatite composites by a simple and eco-friendly method, Ceram. Int. 42 (2016) 2271–2280, https://doi.org/10.1016/j.ceramint.2015.10.021.
[21] M. Mirzaee, M. Vaezi, Y. Palizdar, Synthesis and characterization of silver doped hydroxyapatite nanocomposite coatings and evaluation of their antibacterial and corrosion resistance properties in simulated body fluid, Mater. Sci. Eng. C 69 (2016) 675–684, https://doi.org/10.1016/j.msec.2016.07.057.
[22] R.P. Singh, M. Singh, G. Verma, S. Shukla, S. Singh, S. Singh, Structural analysis of silver doped hydroxyapatite nanopowders by rietveld refinement, Trans. Indian Inst. Met. 70 (2017) 1973–1980, https://doi.org/10.1007/s12666-016-1019-0.

[23] R. Nirmala, F.A. Sheikh, M.A. Kanjwal, J.H. Lee, S. Park, R. Navamathavan, H.Y. Kim, Synthesis and characterization of bovine femur bone hydroxyapatite containing silver nanoparticles for the biomedical applications, J. Nanoparticle Res. 13 (2011) 1917–1927, https://doi.org/10.1007/s11051-010-9944-z.
[24] S.M. Magaña, P. Quintana, D.H. Aguilar, J.A. Toledo, C. Ángeles-Chávez, M.A. Cortés, L. León, Y. Freile-Pelegrín, T. López, R.M.T. Sánchez, Antibacterial activity of montmorillonites modified with silver, J. Mol. Catal. A Chem. 281 (2008) 192–199, https://doi.org/10.1016/j.molcata.2007.10.024.
[25] M. Yamamoto, Y. Kashiwagi, M. Nakamoto, Size-controlled synthesis of monodispersed silver nanoparticles capped by long-chain alkyl carboxylates from silver carboxylate and tertiary amine, Langmuir 22 (2006) 8581–8586.
[26] J.-T. Wu, S.L.-C. Hsu, Preparation of triethylamine stabilized silver nanoparticles for low-temperature sintering, J. Nanoparticle Res. 13 (2011) 3877–3883, https://doi.org/10.1007/s11051-011-0341-z.
[27] A. Bharti, S. Singh, V.K. Meena, N. Goyal, Structural characterization of silver-hydroxyapatite nanocomposite: a bone repair biomaterial, Mater. Today Proc. 3 (2016) 2113–2120, https://doi.org/10.1016/j.matpr.2016.04.116.